crystals

MDPI

Article

Effect of Chromium on Microstructure and Mechanical Properties of Hot-Dip Galvanized Dual-Phase (DP980) Steel

Xuefei Chen [1], Jiawei Liang [1,*], Dapeng Yang [1], Zhiping Hu [2], Xin Xu [2], Xingli Gu [2] and Guangming Xie [1,*]

[1] State Key Laboratory of Rolling and Automation, Northeastern University, Shenyang 110819, China; chenxuefei525@163.com (X.C.); yangdapeng@ral.neu.edu.cn (D.Y.)
[2] Technology Center of Angang Steel Company Limited, 63 Wuyi Road, Anshan 114009, China; huzhiping900401@126.com (Z.H.); ag_xuxin@163.com (X.X.); gu_xingli@126.com (X.G.)
* Correspondence: weeks_liang@163.com (J.L.); xiegm@ral.neu.edu.cn (G.X.)

Abstract: Generally, the addition of Chromium (Cr) into the dual-phase (DP) steels can suppress bainitic transformation. In this work, the continuous hot-dip galvanization of DP980 steel is thermally simulated with various Cr contents of 0/0.3/0.6 wt.%, and the effect of Cr on bainitic transformation and properties of steels is studied. The results indicate that the bainitic transformation is obviously inhibited. The fraction of bainite decreases with the increasing Cr content. The incubation time is prolonged in the 0.6Cr steel with a slower bainitic transformation rate. Compared to that of 0 and 0.3Cr steels, the 0.6Cr steel exhibits a high tensile strength of 1033 MPa and uniform elongation of 9.1% due to the rapid strain-hardening rate. As a result, the mechanical properties of 0.6Cr steel satisfy the requirements of hot-dip galvanized DP980 steel.

Keywords: dual-phase steel; Cr; bainitic transformation; hot-dip galvanization

check for updates

Citation: Chen, X.; Liang, J.; Yang, D.; Hu, Z.; Xu, X.; Gu, X.; Xie, G. Effect of Chromium on Microstructure and Mechanical Properties of Hot-Dip Galvanized Dual-Phase (DP980) Steel. *Crystals* **2023**, *13*, 1287. https://doi.org/10.3390/cryst13081287

Academic Editor: José L. García

Received: 2 August 2023
Revised: 13 August 2023
Accepted: 15 August 2023
Published: 20 August 2023

Copyright: © 2023 by the authors. Licensee MDPI, Basel, Switzerland. This article is an open access article distributed under the terms and conditions of the Creative Commons Attribution (CC BY) license (https://creativecommons.org/licenses/by/4.0/).

1. Introduction

For the comprehensive requirements of reducing the body weight, environment, and safety performance in automobile manufacturing industry, advanced high strength steels (AHSS) have been rapidly developed in recent decades [1]. As the first generation of AHSS, the DP steels are characterized by the soft ferrite matrix and dispersed hard martensite, thus achieving excellent properties with continuous yield, high ultimate tensile strength, and rapid strain hardening at the initial plastic deformation [1–3]. Therefore, DP steels are extensively applicated as structure components for car bodies by the automotive industry.

In addition to mechanical properties, the corrosion resistance of automotive steel is also important to protect the underlying base steel from corrosion and provide longevity. The Zn coating applied to AHSS has the capability of providing cathodic protection and creates a metallurgically bonded zinc–iron barrier layer between steel and environment to improve the corrosion resistance [4]. Therefore, hot-dip galvanization is a necessary process for DP steels, despite this process simultaneously deteriorating the strength [5–7]. The reduction in strength is attributed to the hot-dip galvanized temperature, which is in the range of bainitic transformation and facilitates the generation of bainite. The occurrence of bainite in ferrite and martensite DP steel leads to a decrease in strength, and then the car safety cannot be guaranteed. The change in the martensite volume fraction by 10% causes a decrease in tensile strength of 40 MPa [8,9]. Therefore, inhibiting the bainitic transformation during the hot-dip galvanization process has important significance.

In order to gain sufficient martensite, several alloying elements like Mn, B, and Mo are usually added into DP steel in appropriate amounts [10–12]. Considering the cost, welding performance, and hardenability, about 2 wt.% Mn is usually added to DP980 steel, which can effectively inhibit ferrite and pearlite transformation in quenching [13]. However, it is not sufficient to suppress bainitic transformation during the hot-dip galvanization process and is harmful to galvanization quality [14]. Even though it has been proven in several

studies that this situation can be improved by adding the alloy Mo, the high cost is an unavoidable disadvantage [15–17]. According to previous studies, Cr has a similar effect to Mo, but the cost is significantly lower than Mo [18–20]. This suggests that the alloy element of Cr added to DP steel is a candidate for inhibiting the bainitic transformation during the galvanization process and avoiding strength deterioration.

In summary, the bainite produced during the hot-dip galvanization process results in the degradation of material properties. This degradation can be improved by adding Cr. In this work, three kinds of steels with 0, 0.3, and 0.6 wt.% Cr were used to investigate the effect of Cr on the bainitic transformation and mechanical behaviors. This work will be of practical sense for the future development of high-strength continuous hot-dip galvanized DP steels.

2. Materials and Methods

The chemical composition of experimental steels is shown in Table 1. For the convenience of description, materials were labeled as Cr-free, 0.3Cr, and 0.6Cr, based on the discrepancies in Cr content. The ingots were cast in a vacuum induction furnace and then removed to risers. Ingots were homogenized at 1200 °C in an electric resistance furnace and forged, then cut into four blocks uniformly. After removing the surface oxidation and decarburization layer, the slab was reheated to 1200 °C for 2 h, and then hot-rolled to a thickness of 3.5 mm after 5 passes. The final rolling temperature was 900 °C and the plates were rapidly cooled to 650 °C, then slowly cooled to the room temperature in the furnace in order to simulate the coiling process. Hot-rolled sheets were pickled in 10% hydrochloric acid and then cold-rolled to 1.2 mm in thickness.

Table 1. Chemical composition of experimental steels (wt.%).

Alloys	C	Si	Mn	Al	Nb	Ti	B	Cr	Fe
Cr-free	0.09	0.36	2.29	0.02	0.03	0.03	0.0020	---	Bal.
0.3Cr	0.09	0.35	2.35	0.05	0.02	0.05	0.0020	0.32	Bal.
0.6Cr	0.08	0.43	2.30	0.03	0.02	0.02	0.0017	0.61	Bal.

The experimental process and crucial controlling points of microstructure are shown in Figure 1. The specimens were rapidly heated to the inter-critical region at 10 °C/s. The applied inter-critical temperatures was 780 °C for Cr-free and 0.3Cr steels and 760 °C for 0.6Cr steel, and the isothermal time was 100 s (Process 1 marked as blue). Then, specimens were subjected to slow cooling (about 10 s) to 680 °C, which was chosen based on the practical continuous annealing process. Subsequently, specimens were rapidly cooled and then underwent the hot-dip galvanization process at 460 °C for 20 s (Process 2 marked as red). As shown, the Process 1 was conducted to explore the suitable inter-critical temperature, which is able to generate the same volume fraction proportion of ferrite and austenite to avoid the effect of the different ratios on the bainitic transformation. Process 2 aims to investigate the effect of Cr on the bainitic transformation.

A Tubular furnace and a salt bath furnace were used for the experimental process. The temperature variation was monitored using a K-type thermocouple spot-welded to the surface of the samples. Additionally, the DIL 805A/D dilatometer was applied to simulate the Process 2 in order to investigate the kinetics of bainitic transformation during the hot-dip galvanization process. The sample used for the DIL 805A/D dilatometry test was 10 mm in length (rolling direction) and 4 mm in width. In addition, tensile samples with a gauge width and length of 12.5 mm and 50 mm were used to measure the mechanical properties of experimental steels. The specimens were performed at a tensile rate of 2 mm/min.

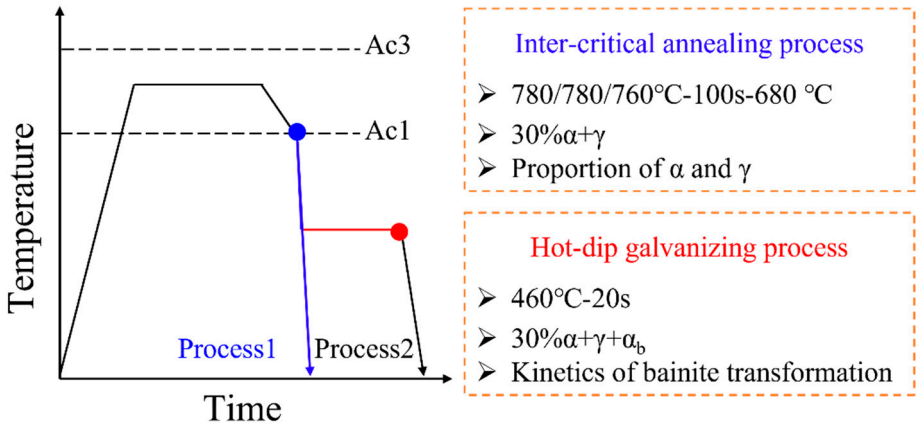

Figure 1. The schemes and the key point.

To investigate the microstructure evolution, samples were subjected to sandpaper polishing and mechanical polishing. Then, samples were prepared via etching with a 4% nital solution for 10 s in order to characterize the microstructure using a field emission scanning electron microscope (SEM). In combination with the microstructure morphology and Image J software with version 1.8.0.112, the statistics of the volume fraction of ferrite after Process 1 was verified. Electro-backscattering diffraction (EBSD) was selected to explore the crystallographic characteristics of the experimental steels at 20 kV with a 0.05 μm step size.

3. Results and Discussion

3.1. Effect of Cr on Microstructure Evaluation

Figure 2 shows the microstructure of three experimental steels after Process 1. As presented, the microstructure is characterized by ferrite and martensite. In the case of Cr-free steel, there are a few elongated ferrite distributed along the rolling direction, as the inhomogeneous distribution of the alloy elements is caused by the rapid heat rate, low inter-critical temperature, and short isothermal time. Compared to Cr-free steel, 0.3Cr and 0.6Cr steels contain equiaxial and coarsening recrystallized ferrite instead of elongated ferrite. Moreover, the volume fractions of ferrite are calculated, and the statistical results show that the ferrite volume fractions are 26 ± 3% for Cr-free steel, 27 ± 1% for 0.3Cr steel and 30 ± 3% for 0.6Cr steel, respectively.

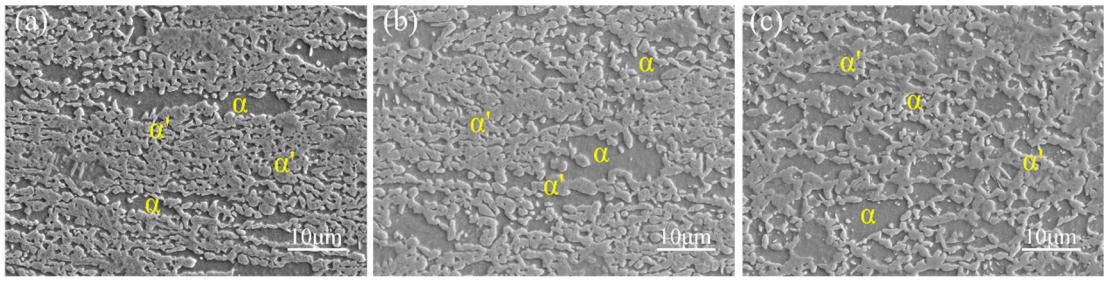

Figure 2. Microstructure of three experimental steels after Process 1. (**a**) Cr-free steel; (**b**) 0.3Cr steel; (**c**) 0.6Cr steel. α: ferrite; α': martensite.

In Figure 3, the microstructure during the hot-dip galvanization process (Process 2) is depicted. There is plenty of bainite in the microstructure of Cr-free and 0.3Cr steels. The bainite morphology is an equiaxed microstructure, which contains island-type M/A constituents in the bainitic ferrite. It is named granular bainite. There is little bainite in 0.6Cr steel. The bainite volume fraction decreases with the increase in Cr content. It demonstrates

that the bainitic transformation is inhibited by the addition of Cr, especially at a content of 0.6 wt.%.

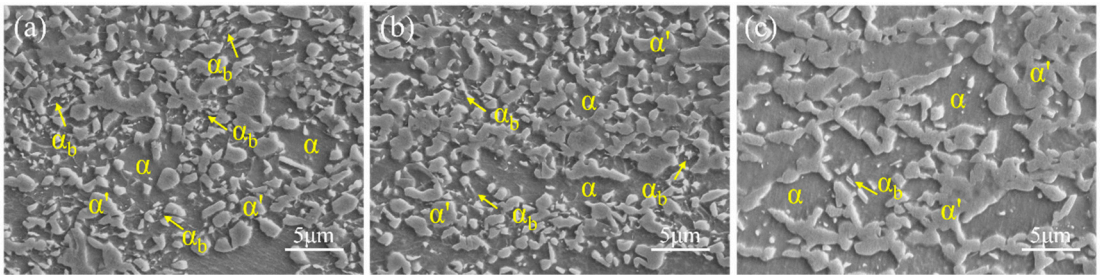

Figure 3. Microstructure of three experimental steels under the Process 2. (**a**) Cr-free steel; (**b**) 0.3Cr steel; (**c**) 0.6Cr steel. α: ferrite; α′: martensite; α_b: bainite.

Additionally, the grain size and the distribution of local misorientation are examined by EBSD. The inverse pole figure (IPF) color maps corresponding to the microstructure obtained by Process 2 and the arrows pointing to the different phase are shown in Figure 4. It can be seen that the grain size of the ferrite of Cr-free steel is large, while the grain size is fine in 0.3Cr steel, as the addition of Cr accelerates the recrystallization of ferrite [21]. As the Cr content increases, the ferrite is subjected to rapid recrystallization and growth during the inter-critical isothermal process. Thus, the large recrystallized ferrite is maintained in the final microstructure. In addition, kernel average misorientation (KAM) maps provide a way to analyze the local scale deformation of experimental steels. In this work, the KAM maps are calculated for the maximum of 3° misorientation. It is shown that the strains in three steels are concentrated at the interface of martensite and bainite and at the boundary of martensite close to the ferrite. The lattice distortion of 0.3Cr steels is more even and regular than that in others due to the fine grain size.

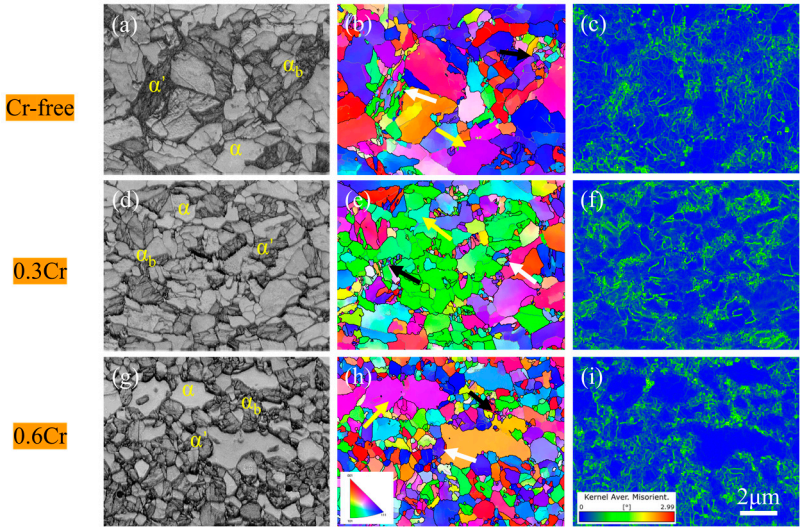

Figure 4. EBSD maps of three experimental steels: (**a**,**d**,**g**) band slop maps, (**b**,**e**,**h**) IPF color maps, and (**c**,**f**,**i**) KAM maps. α: ferrite; α′: martensite; α_b: bainite. black arrow: bainite; white arrow: martensite; yellow arrow: ferrite.

In actuality, the effect of Cr on bainitic transformation may be mainly attributable to the fact that Cr as the ferrite stabilizing element can narrow the austenitic phase region. Moreover, Cr can decrease the diffusion rate of carbon in austenite. In addition, since Cr is a strong carbide-forming element, Cr has a strong connection with carbon, resulting in difficulties in moving the phase interface. As the above factors are keys aspect of the

kinetics of bainitic transformation, it is necessary to investigate the kinetics of Cr on bainitic transformation. This is analyzed in detail in Section 3.2.

When the austenite transforms to bainite or martensite, the crystal structure changes from face-centered cubic (fcc) to body-centered cubic (bcc). Thus, the lattice volume increases and the density changes from 0.74 to 0.68. The analysis of the Gibbs free energy between fcc and bcc indicates that the Gibbs free energy decreases following the increase in Cr content. Considering the storage energy (400 J/mol) for bainitic formation, Gibbs free energy is −1053.43 J/mol for Cr-free steel, −1038.63 J/mol for 0.3Cr steel, and −1019.84 J/mol for 0.6Cr steel, respectively.

To further analyze the effect of Cr on the kinetics of bainitic transformation, the dilatometer was selected to simulate the hot-dip galvanization process, because the dilatometric curve can reflect the variation of lattice volume and the change in length of dilatometric result can be converted to the volume fraction of bainite, according to the law of leverage [22]. According to the bainite incomplete transformation, bainitic transformation will cease when the carbon content in austenite reaches the critical content corresponding to the T_0 temperature when the free energy of bainite becomes less than that of austenite with the same composition. The rate of bainitic transformation tends to slow down with the extension of isothermal time. At this point, the dilatometric curve tends to be horizontal, which means the bainitic transformation reaches the stasis stage.

Figure 5 illustrates the dilatometric results of three experimental steels during the hot-dip galvanization process. As shown, austenite does not decompose before the isothermal holding process, since there is no change in the slope of the dilatometric curves. During the isothermal process at 460 °C, the increase in dilatation indicates the occurrence of bainitic transformation. Hence, there is an obvious bainitic transformation of Cr-free and 0.3Cr steels but only a small increase in the dilatation of 0.6Cr steel. Subsequently, the unstable retained austenite transforms to martensite during cooling. The start temperature of martensite (Ms) increases with the increase in Cr content. As shown in Figure 5b, there is no incubation period for Cr-free and 0.3Cr steels, while the incubation time of 0.6Cr steel is prolonged to 1.5 s. In addition, at the initial stage of the bainitic transformation (within the isothermal time of 10 s), the rate of bainitic transformation of Cr-free and 0.3Cr steels are more than twice as fast as that of 0.6Cr steel. As the isothermal time is extended, the rate of the bainitic transformation of Cr-free and 0.3Cr steels decreases, while the rate of 0.6Cr steel is constant. Figure 6 presents the volume fractions of phases based on the dilatometric results to express the variation in volume fractions. As presented, the Cr-free and 0.3Cr steels have a higher volume fraction (about 50%) than that of 0.6Cr steel (about 35%). A large amount martensite is present in 0.6Cr steel compared to that in Cr-free and 0.3Cr steels. Therefore, it can be concluded that the addition of 0.6 wt.% Cr inhibits the bainitic transformation effectively.

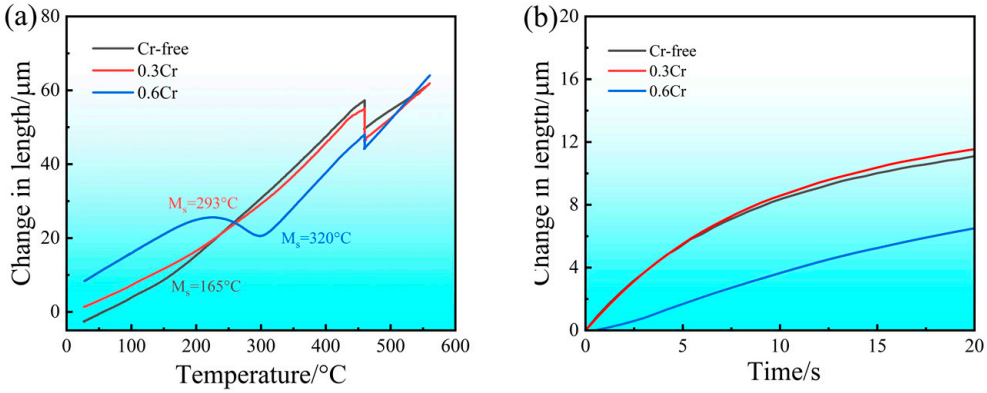

Figure 5. Dilatometric results of three experimental steels during the hot-dip galvanization process. (**a**) dilatation as a function of temperature; (**b**) dilatation as a function of time.

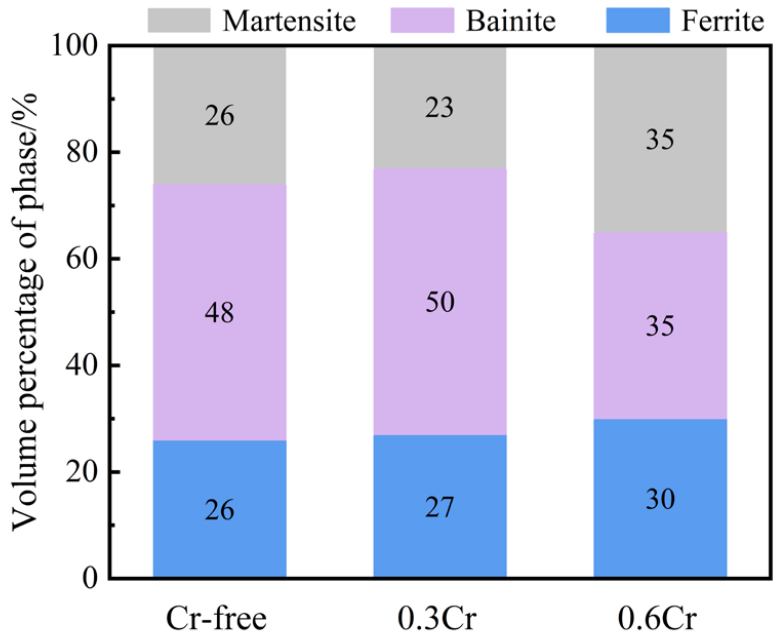

Figure 6. Volume fraction of the phases in three experimental steels after the isothermal process at 460 °C for 20 s.

In addition, the effect of Cr on the bainitic transformation at 460 °C for 20 s was investigated using a modified Johnson–Mehl–Avrami–Kolmogorov (JMAK) model, specifically [23,24]. It is expressed as follows:

$$f = 1 - \exp(-kt^n) \quad (1)$$

where f is the fraction of bainite; k and n are the phase transformation kinetics parameters; and t is the time from the start of bainitic transformation to the end.

Figure 7 presents the results of bainitic transformation kinetics calculated via the modified JMAK model, and the corresponding values are displayed in Table 2. The results indicate that the actual dilatometric data and the fitting curve have a strong correlation, since the fitting correlation coefficients are 0.99 for each curve. Additionally, it should be noted that the constant n of Cr-free and 0.3Cr steels are 0.83 and 0.79 but is 1.16 for 0.6Cr steel. Since the constant n is a morphology-dependent constant and an indicator of the transformation mechanism, the results suggest that the nucleation rate of bainite decreases as time is extended and the bainite of Cr-free and 0.3Cr steels grows in one dimension. In this situation, the bainite ferrite nucleates at the grain boundary and the lengthening of bainitic ferrite lath is faster than the thickness. For 0.6Cr steel, bainite grows in the form of appreciable initial volume particles [25]. Moreover, the value of k is an important parameter to reflect the rate of bainitic transformation. The value of k is 0.02 for 0.6Cr steel, which is lower than that of 0.11 and 0.12 for Cr-free and 0.3Cr steels, respectively. The smaller value of 0.6Cr steel indicates a more efficient bainitic transformation and a longer time for the completion of the bainitic transformation. Unlike the martensite transformation without any diffusion of atoms, carbon redistributes into the untransformed austenite during the formation of bainite, even though the generation of the sub-unite is displacive. Due to the high isothermal galvanized temperature of 460 °C, carbon in the austenite diffuses rapidly, while the addition of Cr decreases the diffusion rate of carbon. As a result, the bainitic transformation is retarded. Therefore, the addition of 0.6 wt.% Cr reduces the volume fraction of bainite and decreases the bainitic transformation rate at the initial stage.

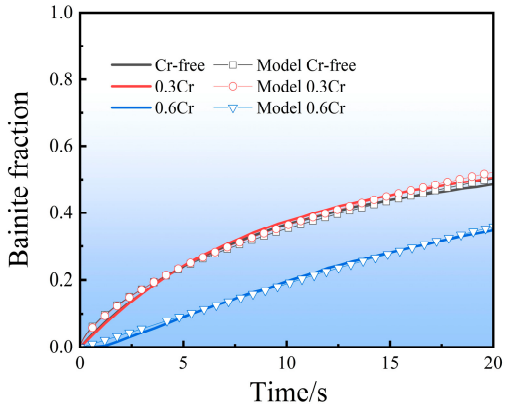

Figure 7. Kinetics of bainitic transformation of three experimental steels at 460 °C for 20 s.

Table 2. Values of the modified JMAK kinetic parameters.

Alloys	n	k	R
Cr-free	0.83	0.11	0.99
0.3Cr	0.79	0.12	0.99
0.6Cr	1.16	0.02	0.99

3.2. Effect of Cr on Mechanical Properties

The engineering stress–engineering strain curves are illustrated in Figure 5a, and the detailed values of the properties are shown in Table 3. As presented, the higher the addition of Cr, the higher the tensile strength of the steel. Moreover, the 0.6Cr steel has the highest tensile strength of 1033 MPa, which is higher than Cr-free and 0.3Cr steels by 7% and 14%. Additionally, three steels show the typical continuous yield characteristics of dual-phase steel. The yield strengths of three experimental steels are 545 MPa, 623 MPa, and 592 MPa for Cr-free, 0.3Cr, and 0.6Cr steels, respectively. Even though the highest tensile strength is present in 0.6Cr steel, there is almost no loss of total elongation due to high uniform elongation. Consequently, it can be concluded that the addition of 0.6Cr enhances the properties sufficiently to satisfy the requirements of DP980 steel.

Table 3. Mechanical properties of experimental steels.

Alloys	YS/MPa	TS/MPa	TEL/%	UEL/%	YS/TS
Cr-free	545	910	12.3	8.7	0.60
0.3Cr	623	980	10.0	6.7	0.63
0.6Cr	592	1033	11.2	9.1	0.57

YS: yield strength; TS: tensile strength; TEL: total elongation; UEL: uniform elongation.

As is well known, the tensile strength of dual-phase steel has a directly proportional relationship with the volume fraction of ferrite and martensite, and it generally increases with the increase of martensite volume fraction, depending on the law of mixture [26]. When the microstructure consists of ferrite, martensite, and bainite, the strength not only has a close relationship with the martensite volume fraction but also the volume fraction of bainite. As a result, the tensile strength is easily weakened due to the presence of bainite. In this study, however, the bainite is effectively inhibited via the addition of 0.6 wt.% Cr during the galvanization process. Therefore, 0.6Cr steel has the highest tensile strength. In addition, the yield strength, which obeys the Hall–Petch relationship, increases with the decrease in grain size [27]. Moreover, for DP steel, the yield strength has a strong relationship with the strength of ferrite. Based on the Hall–Petch relationship, the ferrite strength increases as the grain size decreases. Therefore, due to the small grain size, 0.3Cr steel has the highest

yield strength of the three experimental steels. The uniform elongation will be interpreted in combination with the strain hardening behavior in the following section.

Therefore, the Hollomon and modified Crussard–Jaoul (C–J) models were used in this work to investigate strain hardening behavior [28,29]. Both are expressed as follows:

$$\varepsilon = \varepsilon_0 + c\sigma^m \tag{2}$$

where ε_0 is the initial true stain, c is a constant, and m is the strain hardening index.

$$ln(d\sigma/d\varepsilon) = (1-m)ln\sigma - lnkm \tag{3}$$

where σ and ε are the true stress and strain, respectively. k is a parameter with material constants.

As presented in Figure 8b, there are two strain hardening stages. At the initial stage, the strain hardening indexes (m_1) are 3.90, 3.58, and 2.43 for Cr-free, 0.3Cr, and 0.6Cr steels, respectively. This signifies that 0.6Cr steel has the highest strain hardening capability during first stage. With the increase in cumulative deformation, the strain hardening behavior turns to the second stage and the strain hardening rate reduces gradually. During the second stage, the strain hardening indexes (m_2) are 12.11, 12.75, and 11.76 for Cr-free, 0.3Cr, and 0.6Cr steels, respectively. The strain hardening rate of 0.6Cr steel remains higher than that of Cr-free and 0.3Cr steel. Additionally, the transition strains (ε_{tr}) from the first stage to the second stage are 0.8, 0.6, and 0.8 for Cr-free, 0.3Cr, and 0.6Cr steels. This indicates the similar coordinated deformation capability of the three experimental steels.

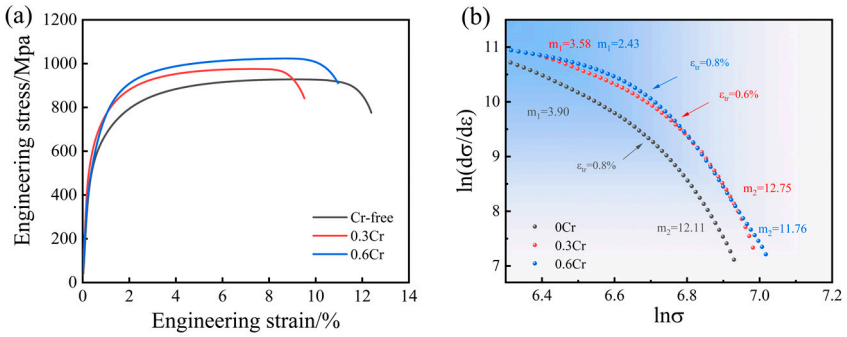

Figure 8. (**a**) Engineering stress–strain curves; (**b**) the modified C–J analysis of in $ln(d\sigma/d\varepsilon)$ vs. $ln(\sigma)$.

According to the results of previous studies [28–30], during the initial stage, generally, plastic deformation occurred only in ferrite, while the martensite retained elastic deformation. The rapid accumulation and multiplication of dislocation caused by the martensitic shear transformation led to the high strain hardening rate during the initial deformation stage [9]. Hence, it can be inferred that martensite transformation contributed to the rapid strain hardening behavior. However, in this study, massive bainitic transformation occurs in Cr-free and 0.3Cr steels, while it is strongly inhibited by the addition of 0.6 wt.% Cr. In general, the density of mobile dislocations caused by bainitic transformation is lower than that produced by martensite transformation. Thus, this indicates that the existence of substantial bainite in Cr-free and 0.3Cr steels results in a slower strain hardening rate than that of 0.6Cr steel at the initial stage. Therefore, the strain hardening index of m_1 for 0.6Cr steel is smaller than that of the other steels. As the increase in deformation, the deformation transfers from the ferrite to the martensite or bainite. Subsequently, the ferrite and martensite begin to deform plastically together in the second stage. The plastic deformation of martensite or bainite starts almost simultaneously, which is demonstrated by the similar transition strain shown in the results of the C–J model. As the movement of dislocation is limited by martensite or bainite, the dislocation is piled up, which results in the gradual decrease in strain hardening rate. Thus, the value of m_2 is lower than m_1

during the second stage. As the results show, during the second stage, 0.6Cr steel still exhibits a relatively faster strain hardening rate than the others. This can be attributed to the fact that the large amount of high-strength martensite effectively blocks the dislocation movement. In addition, 0.6Cr steel has the higher uniform elongation than the others, which is dominated by strain hardening. As a consequence, 0.6Cr steel achieves high strength properties without loss of uniform elongation.

4. Conclusions

In this work, to inhibit the bainitic transformation of DP steel during the hot-dip galvanization process, DP steels with different Cr contents were designed to investigate the effect of Cr on bainitic transformation. Moreover, the mechanical behaviors were also discussed in detail. The main conclusions are as follows:

1. Compared to Cr-free steel, the bainitic volume fraction of 0.6Cr is significantly decreased. Moreover, Cr delays the incubation time and decreases the rate of the bainitic transformation.
2. The tensile strength and yield strength are improved by the addition of 0.6 wt.% Cr without a loss of uniform elongation.
3. The mechanical properties of 0.6Cr steel achieve a tensile strength of 1033 MPa and a uniform elongation of 9.1%, which satisfies the requirement of hot-dip galvanized DP980 steel.

Author Contributions: Writing—original draft preparation and review, X.C.; writing—review and editing, J.L.; supervision, G.X. and D.Y.; project administration, X.G. and X.X.; investigation, Z.H. All authors have read and agreed to the published version of the manuscript.

Funding: This work was supported by the National Nature Science Foundation (No. 52101128, 52274378, and 51774085), National Key R&D Program (No. 2018YFE0306102), Postdoctoral Science Foundation (No. 2022M710021), Liaoning Province Excellent Youth Foundation of China (No. 2020-YQ-03), the Open Research Fund from the State Key Laboratory of Rolling and Automation of Northeastern University (No. 2020RALKFKT009), and Postdoctoral Research Fund of Northeastern University of China of China (No. 20220202).

Data Availability Statement: Data is contained within the article.

Conflicts of Interest: The authors declare no conflict of interest.

References

1. Zhao, J.W.; Jiang, Z.Y. Thermomechanical processing of advanced high strength steels. *Prog. Mater. Sci.* **2018**, *94*, 174–242. [CrossRef]
2. Bouaziz, O.; Zurob, H.; Huang, M.X. Driving force and logic of development of advanced high strength steels for automotive applications. *Steel Res. Int.* **2013**, *84*, 937–947. [CrossRef]
3. Park, K.S.; Park, K.T.; Lee, D.L.; Lee, C.S. Effect of heat treatment path on the cold formability of drawn dual-phase steel. *Mater. Sci. Eng. A* **2007**, *449–451*, 1135–1138. [CrossRef]
4. Petit, E.J.; Grosbety, Y.; Aden-Ali, S.; Gilgert, J.; Azari, Z. Microstructure of the coating and mechanical properties of galvanized chromium-rich martensitic steel. *Surf. Coat. Technol.* **2010**, *205*, 2404–2411. [CrossRef]
5. Mintz, B. Hot dip galvanising of transformation induced plasticity and other inter-critically annealed steels. *Int. Mater. Rev.* **2013**, *46*, 169–197. [CrossRef]
6. Pan, E.; Di, H.; Jiang, G.; Bao, C. Effect of Heat Treatment on Microstructures and Mechanical Properties of Hot-Dip Galvanized DP Steels. *Acta Met. Sin. Engl. Lett.* **2014**, *27*, 469–475. [CrossRef]
7. Lin, K.C.; Chu, P.W.; Lin, C.S.; Chen, H.B. Galvanizing and Galvannealing Behavior of CMnSiCr Dual-Phase Steels. *Met. Mater. Trans. A.* **2013**, *44*, 2690–2698. [CrossRef]
8. Fonstein, N.; Jun, H.J.; Huang, G. Effect of bainite on mechanical properties of multiphase ferrite-bainite-martensite steels. *Mater. Sci. Technol.* **2011**, *1*, 333–341.
9. Kumar, A.; Singh, S.B.; Ray, K.K. Influence of bainite/martensite-content on the tensile properties of low carbon dual-phase steels. *Mater. Sci. Eng. A* **2008**, *474*, 270–282. [CrossRef]
10. Schemmann, L.; Zaefferer, S.; Raabe, D.; Friedel, F.; Mattissen, D. Alloying effects on microstructure formation of dual phase steels. *Acta Mater.* **2015**, *95*, 386–398. [CrossRef]

11. Lai, Q.; Bouaziz, O.; Gouné, M.; Perlade, A.; Bréchet, Y.; Pardoen, T. Microstructure refinement of dual-phase steels with 3.5 wt% Mn: Influence on plastic and fracture behavior. *Mater. Sci. Eng. A* **2015**, *638*, 78–89. [CrossRef]
12. Douguet, P.; Da Rosa, G.; Maugis, P.; Drillet, J.; Hoummada, K. Effect of boron segregation on bainite nucleation during isothermal transformation. *Scr. Mater.* **2022**, *207*, 114286. [CrossRef]
13. Taylor, M.D.; Choi, K.S.; Sun, X.; Matlock, D.K.; Packard, C.E.; Xu, L.; Barlat, F. Correlations between nanoindentation hardness and macroscopic mechanical properties in DP980 steels. *Mater. Sci. Eng. A* **2014**, *597*, 431–439. [CrossRef]
14. Liu, H.; Li, F.; Shi, W.; Swaminathan, S.; He, Y.; Rohwerder, M.; Li, L. Challenges in hot-dip galvanizing of high strength dual phase steel: Surface selective oxidation and mechanical property degradation. *Surf. Coat. Technol.* **2012**, *206*, 3428–3436. [CrossRef]
15. Wang, L.Y.; Wu, Y.X.; Sun, W.W.; Bréchet, Y.; Brassart, L.; Arlazarov, A.; Hutchinson, C.R. Transitions in the strain hardening behaviour of tempered martensite. *Acta Mater.* **2021**, *221*, 117397. [CrossRef]
16. Xia, Y.; Miyamoto, G.; Yang, Z.G.; Zhang, C.; Furuhara, T. Direct measurement of carbon enrichment in the incomplete bainite transformation in Mo added low carbon steels. *Acta Mater.* **2015**, *91*, 10–18. [CrossRef]
17. Han, Q.H.; Kang, Y.L.; Zhao, X.M.; Lü, C.; Gao, L.F. Microstructure and Properties of Mo Microalloyed Cold Rolled DP1000 Steels. *J. Iron Steel Res. Int.* **2011**, *18*, 52–58. [CrossRef]
18. Han, Y.; Kuang, S.; Liu, Y.S.; Jiang, Y.H.; Liu, G.H. Effect of Chromium on Microstructure and Mechanical Properties of Cold Rolled Hot-dip Galvanizing DP450 Steel. *J. Iron Steel Res. Int.* **2015**, *22*, 1055–1061. [CrossRef]
19. Bracke, L.; Xu, W. Effect of the Cr Content and Coiling Temperature on the Properties of Hot Rolled High Strength Lower Bainitic Steel. *ISIJ Int.* **2015**, *55*, 2206–2211. [CrossRef]
20. Irie, T.; Satoh, S.; Hashiguchi, K.; Takahsahi, I.; Hashimoto, O. Metallurgical Factors Affecting the Formability of Cold-rolled High Strength Steel Sheets. *Trans. Iron Steel Inst. Jpn.* **1981**, *21*, 793–801. [CrossRef]
21. Silva Filho, J.F.D.; Oliveira, C.A.S.D.; Fonstein, N.; Girina, O.; Miranda, F.J.F.; Drumond, J.; Serafim, E.A.; Afonso, C.R.M. Effect of Cr Additions on Ferrite Recrystallization and Austenite Formation in Dual-Phase Steels Heat Treated in the Intercritical Temperature Range. *JMR* **2016**, *19*, 258–266. [CrossRef]
22. Tsai, S.-P.; Su, T.-C.; Yang, J.-R.; Chen, C.-Y.; Wang, Y.-T.; Huang, C.-Y. Effect of Cr and Al additions on the development of interphase-precipitated carbides strengthened dual-phase Ti-bearing steels. *Mater. Des.* **2017**, *119*, 319–325. [CrossRef]
23. Fang, L.; Wood, W.E.; Atterdge, D.G. Identification and range quantification of steel transformation products by transformation kinetics. *Met. Mater. Trans. A* **1997**, *28*, 5–14. [CrossRef]
24. Caballero, F.G.; Santofimia, M.J.; Gracia-Mateo, C. Time-temperature-transformation diagram within the bainitic temperature range in a medium carbon steel. *Mater. Trans.* **2004**, *45*, 3272–3281. [CrossRef]
25. Quidort, D.; Breche, Y.J.M. A model of isothermal and non isothermal transformation kinetics of bainite in 0.5% C steels. *ISIJ Int.* **2002**, *42*, 1010–1017. [CrossRef]
26. Hupper, T.; Endo, S.; Ishikawa, N. Effect of volume fraction of constituent phases on the stress-strain relationship of dual-phase steels. *ISIJ Int.* **1999**, *39*, 288. [CrossRef]
27. Ramazani, A.; Mukherjee, K.; Prahl, U.; Bleck, W. Transformation-Induced, Geometrically Necessary, Dislocation-Based Flow Curve Modeling of Dual-Phase Steels: Effect of Grain Size. *Met. Mater. Trans. A* **2012**, *43*, 3850–3869. [CrossRef]
28. Zhang, J.; Di, H.; Deng, Y.; Misra, R.D.K. Effect of martensite morphology and volume fraction on strain hardening and fracture behavior of martensite–ferrite dual phase steel. *Mater. Sci. Eng. A* **2015**, *627*, 230–240. [CrossRef]
29. Xiong, Z.P.; Kostryzhev, A.G.; Stanford, N.E.; Pereloma, E.V. Microstructures and mechanical properties of dual phase steel produced by laboratory simulated strip casting. *Mater. Des.* **2015**, *88*, 537–549. [CrossRef]
30. Hung, T.T.; Gou, R.B.; Dan, W.J.; Zhang, W.G. Strain-hardening behaviors of dual phase steels with microstructure features. *Mater. Sci. Eng. A* **2016**, *672*, 88–97. [CrossRef]

Disclaimer/Publisher's Note: The statements, opinions and data contained in all publications are solely those of the individual author(s) and contributor(s) and not of MDPI and/or the editor(s). MDPI and/or the editor(s) disclaim responsibility for any injury to people or property resulting from any ideas, methods, instructions or products referred to in the content.